The 14th World Conference on Earthquake Engineering
October 12-17, 2008, Beijing, China

NUMERICAL STUDIES ON RESIDUAL SEISMIC CAPACIY OF RC FREMES WITH UNREINORCED BLOCK WALL BASED ON THEIR CRACK PATTERNS

M.A. DASTAN[1], M. YEKRANG NIA[2] and A. VAFAI[3]

[1]MSc student, Sharif university of technlogy, Tehran, Iran ma.dastan@yahoo.com
[2]MSc student, Sharif university of technlogy, Tehran, Iran civil_yekrang@yahoo.com
[3]Professor, Sharif university of technology, vafai@sharif.edu

SUMMARY

In this study, two Concrete Block (CB) infilled reinforced concrete frames which had been experimentally investigated before [Nakano et al., 2004] are numerically simulated to develop pre- and post-earthquake seismic evaluation method. In these simulations, full scale, one bay, single story specimens having different axial loads in columns are analyzed under cyclic and push-over loading. Then, the contribution of Unreinforced Masonry (URM) walls to overall behavior is examined. Parameters including stiffness, ductility, strength, crack patterns and widths in walls and frames which may be of great significance in terms of post-event assessment are also studied. In this paper, the relationship between observed damage and seismic performance mainly focusing on crack width in URM walls is discussed by means of smeared crack, homogenized, isotropic modeling.

KEYWORDS

masonry infill, RC frame, residual capacity, crack width, seismic capacity reduction factor

INTRODUCTION

Regarding the fact that annual death toll of earthquakes in Iran reaches to 4000 people and a large number of people who lost their lives in earthquakes, inhabited in unreinforced masonry houses, seismic assessment of these structures in order to perform an optimized method and quantity of rehabilitation, seems to be a challenge. A considerable number of demolished structures are located in earthquake-prone areas and hence had probably experienced some earthquakes in the past. So they have undergone some damages in their load-bearing and non load-bearing elements. In that case, determination of residual capacity of these buildings is an invaluable key to decide whether a typical building is worth rehabilitation or not. Since simplicity and feasibility of each assessment process should be an indispensable factor, the required parameters for assessing a building should be kept as less as possible and easily acquirable. In response to this need, a method proposed by Choi et al. 2005 can assess the residual seismic capacity of reinforced concrete frames with unreinforced block wall based on their crack widths. Since by now, few investigations have been made on quantity-oriented seismic assessments of concrete frame with masonry infill panels.

SELECTION OF THE MODELS

To satisfy the objective of this study, and in order to have an experimental work to verify the results with them, the models are exactly the same as Nakano's et al. 2004.

Figure 1 shows the simulated models. To determine the effect of infill wall on different aspects of the combined system's behavior, the bare frame was modeled first. By exerting different amounts of vertical loads, the models represent bare and infilled frames in different stories. The axial loads applied in each column are 720 KN ($4N/mm^2$) and 180 KN ($1N/mm^2$) for simulating the 1st and the 4th story, respectively. Models B1, B4, I1 and I4 represent Bare and Infill frames of the 1st and the 4th story, respectively.

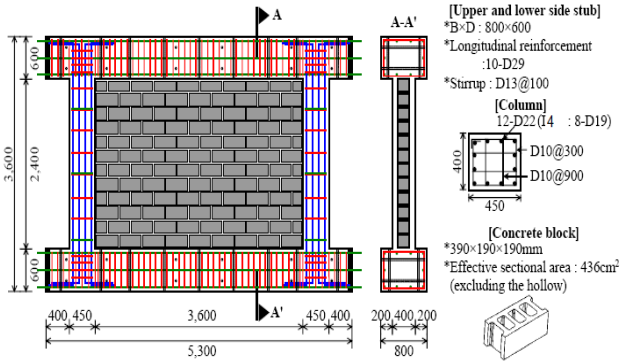

Figure 1 Details of experimental models

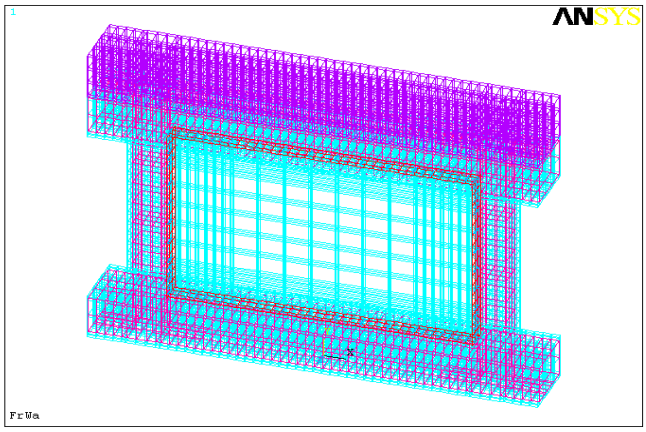

Figure 2 Numerical model

DESCRIPTION OF THE MODEL

In this study, the behavior of the aforementioned specimens is analyzed with the aid of Implicit Macro finite element models. Although macro modeling is broadly used in RC members and proved its robustness, due to orthotropic nature of masonry, continuum modeling of masonry members seems to lead to un-conservative results. However, many theoretical and numerical works to improving the homogenization approach in the field of masonry have been implemented and they have been satisfactorily successful [Ramalho et al., 2007, Lopez et al., 1999, Lee et al., 1996, Lourenco, 1996, Fuschi et al., 1995, Seim, 1994, Abu-Lebdeh and Voyiadjis, 1993, Stevens and Liu, 1992, Lotfi and Shing, 1991, Yazdani and Schreyer, 1990, Schmidt, 1989, Del Piero, 1989, Hsieh et al. ,1988, Liauw and Lo, 1988, Willam et al.,1987, Rots and Borst, 1987, Dhanasekar and Page, 1986, Dhanasekar et al., 1985, Samarazinghe et al., 1981, Litton, 1974]. The element used for simulating concrete frame and infill wall is 8-node first order SOLID65. This element can model smeared cracks and is capable of modeling smeared reinforcing in three directions with different orientations. SOLID 65 incorporates the constitutive model for triaxial behavior of concrete after [Williams and Warnke, 1975]. The rebars can tolerate tension and compression, but not shear bending. It can model tensional cracks in three orthogonal planes and crushing. When the element is cracked or crushed, a small amount of stiffness is added to the element for numerical stability.

Since the smeared reinforcing option in SOLID65 may cause some inaccuracies [Tavarez 2001] especially in flexural behavior, the reinforcement has been exactly modeled. For simulating the reinforcing bars and stirrups both in columns and beams, LINK8 was used. This element can transmit only axial forces and works as a truss member.

The average modulus of elasticity and compressive and tensile strength of concrete is 2.18E+04, 26.7 and 1.66 MPa respectively. For constructing the compressive uniaxial stress-strain curve of concrete, the model proposed by Gere and Timoshenko, 1997 was used. For steel reinforcement, the modulus of elasticity and yield strength is 1.94E+05 and 442 MPa respectively. The behavior of steel was assumed to be bilinear with the zero stiffness in the second phase. In order to model the masonry infill, the mechanical properties of block prism with the elastic modulus of 2.21E+04 MPa and compressive strength of 10.3 MPa were assigned to the homogeneous, isotropic infill. The stress-strain behavior of masonry infill was assumed to follow the formula proposed by [Kent and Park 1971]:

$$\frac{f}{f_m} = 2\frac{\varepsilon}{\varepsilon_m} - (\frac{\varepsilon}{\varepsilon_m})^2 \quad (1)$$

In which f_m and ε_m are the maximum strength and its related strain, respectively.

Modeling of interface between reinforcing and the surrounding concrete is one of the most challenging parts in RC numerical simulation. The assumption that reinforcing bars cannot "barely" pull out from the concrete seems to be a logical one [Moseafaei et al., 2004, Fanning, 2001, Kachlakev et al., 2001]. It is obvious that when the reinforcing bar is going to pull out from its surrounding concrete, it scoops a little concrete trapped within the jags of the bar which participates in force bearing action. So, pure sliding of reinforcing bars does not occur in RC members. In doing so, the nodes on the reinforcing bar elements and their adjacent nodes of concrete elements have been merged to form a common node, hence defining a full bond. In this case, there is no need for defining a contact mechanism between these two types of elements. The nodes belonging to beams and columns at their intersection areas are also merged to form a uniform behavior.

The interface between CB wall and RC frame as modeled with node-to-surface contact pairs. The mechanical properties of mortar were applied to contact elements. The contact pair has frictional Mohr-Columb behavior with frictional coefficient of 0.8.

Since the infill wall consisted of hollow bricks, an equivalent net thickness of the infill wall should be incorporated in the numerical simulation. For this purpose, the wall thickness in this analysis can be calculated as:

467 cm^2/39 cm=12 cm (2)

LOADING MECHANISM

Cyclic lateral loads are applied to each specimen through a loading beam tightly fastened to a specimen. Figure 3 shows the loading history. The peak drift angle R is defined as lateral displacement / column height. Since the mechanism of loading is quasi static, the rate of loading is of no importance; hence, the history of loading is plotted with R in horizontal axis. Because the objective of this analysis is studying the behavior of frame-infill system which encounters high nonlinearities, the input load is displacement not force. As shown in Figure 3, 2.5 cycles for each peak drift are imposed to eliminate one sided progressive failure (unsymmetrical failure pattern in positive and negative loadings). The 0.4% drift imposed after the drift of 1.0% is to investigate the effect of small amplitude after large deformations. (i.e. aftershocks) In addition to cyclic loading, a push-over analysis was performed for each model to better monitor the crack pattern and stress distribution.

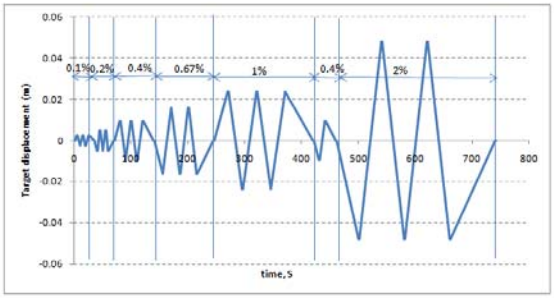

Figure 3 Loading history

ANALYSES RESULTS

Figure 4 (a) and (b) shows the crack pattern of each specimen at UX=1.6 mm and 9.3 mm in the push-over analysis, respectively. As can be observed from the figure, the cracks in columns are horizontal at both ends; indicating flexural failure. In the next stages, however, shear inclined cracks tend to propagate into the columns center which is the main cause of ultimate failure of the system. As it is obvious, the cracks in the windward

column are propagated more rapidly due to tensional forces. In the infill, diagonal inclined cracks representing the step diagonal cracking in the experiment widens in the following load stages. The cracks at the corner of the infill are not due to toe crushing which is the final failure modes of infilled frames, but the tensile cracks are due to Poisson effect caused by stress concentration in those regions.

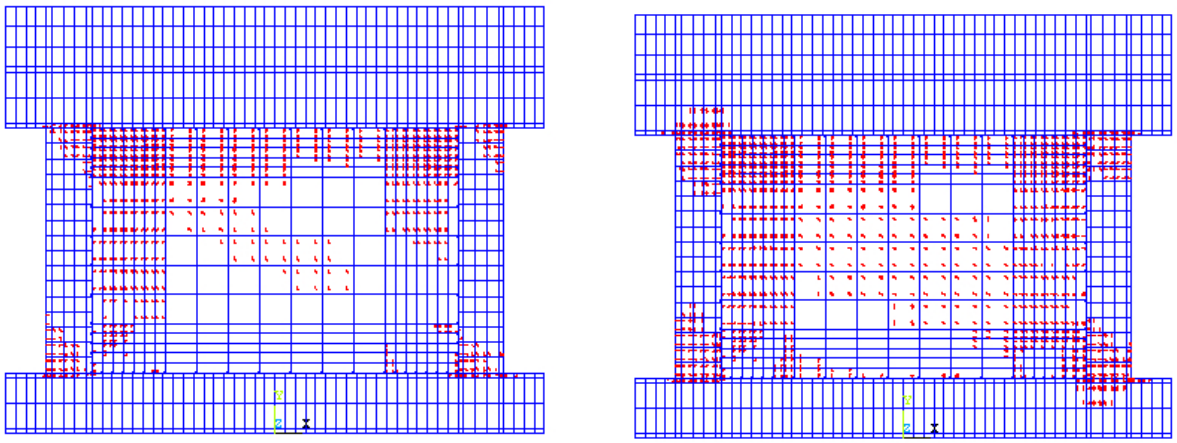

(a) **(b)**

Figure 4 crack pattern for specimen I4 in 1.6 mm and 9.3 mm

THE RELATION OF LATERAL LOAD AND DRIFT ANGLE

Figure 5 shows the hysteretic graph of specimen I1. The relation of maximum force generated in each specimen, ductility, and the differences with the results from the previously done experiment are briefly discussed below.

In the preliminary analyses, the stiffness of the system was greater than experimental specimens. After altering different input parameters of the models, the difference can be justified by the fact that merging the rebars' nodes and the surrounding concrete, can lead to a huge stiffness and ductility of the system [Ramalho et al., 2007]. Calibration processes are mainly focusing on changing the modulus of elasticity and accordingly, the strength of materials. It is obvious from Figure 5 that the model is capable of showing the behavior of the experimental specimens. The only difference is that pinching behavior cannot be observed in the numerical model. The main cause of this situation may be the fact that the bed joint opening does not close on release of the lateral cyclic load or displacement [Senthivel et al., 2006].

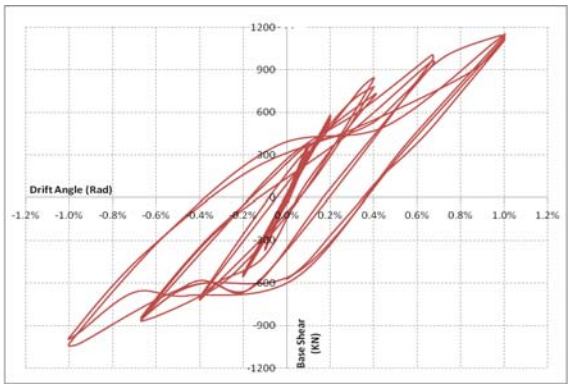

Figure 5 Hysteretic behavior of model I1

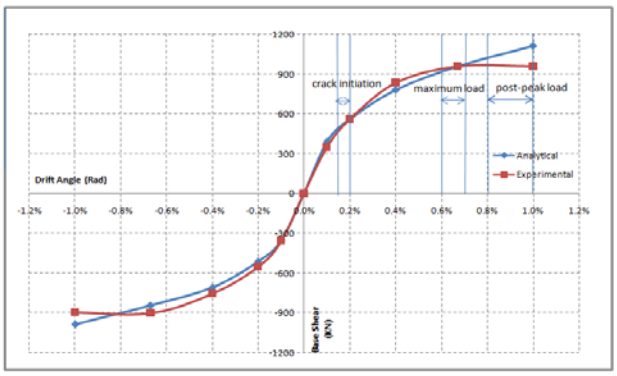

Figure 6 Comparison of numerical and experimental upper and lower band in hysteretic curve of model I1

In Figure 6, the behavior of the numerical and experimental models has been compared and the proposed drifts for crack initiation, peak and post-peak loads based on experiments done by Chen 2003 and Mehrabi et al., 1996

are shown. It is obvious from the Figure 6 that the model is capable of predicting the stiffness and ductility of the model. Very good agreements between the analytical and experimental results have been obtained except in the post-peak region. While in the experiment, the specimens showed softening behavior, in the numerical model, the base shear continues to increase. This is mainly because in implicit analysis in Ansys, modeling of softening behavior is not possible. The other factor contributing in this inaccuracy is that in the experiment, the main cause of failure at the end of loading was:

1. Rapidly opening of shear cracks (shear sliding) at the base of the leeward column (compression column)
2. Propagation of stair-stepped diagonal cracks in the masonry infill [Nakano et al., 2004].

In the numerical analysis, on the one hand, shear sliding in columns cannot be modeled; on the other hand, due to homogeneity and isotropy of the infill, sliding of bed joints cannot occur; Only some diagonal tension cracking were observed. These resulted in development of confined diagonal compression strut in the infill and therefore much higher lateral strength. This problem was attributed to the inefficiency of the smeared crack concept for modeling of the shear failure. This problem may be resolved to somehow by defining some discontinuities with the aid of contact element [Shing et al., 2002, Mehrabi et al., 1997]. In this article, by attributing crushing capability to the 25% height of the columns at both ends, the falling branch of the hysteretic curves was obtained.

After attributing crushing capability to the ends of the columns, the results of push-over analysis are according to Figures 8 and 9 for the 1st and the 4th story, respectively. As can be seen from the two figures and when compared to the bare frame, the infill wall is more effective in 4th story which can improve the strength up to 3 times; while in the 1st story, the strength of the system increases 2 times in the presence of the infill. Also the ductility of the system in 4th story is more than in 1st story.

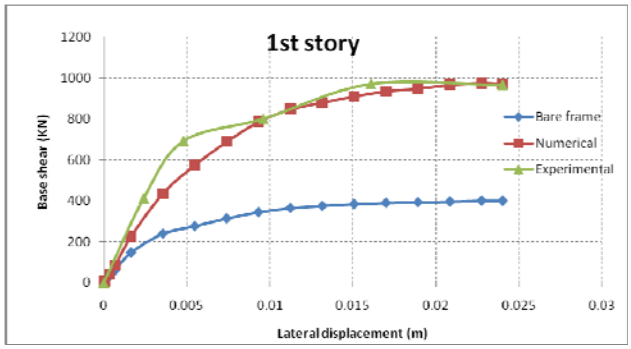

Figure 8 Push over results of 1st story

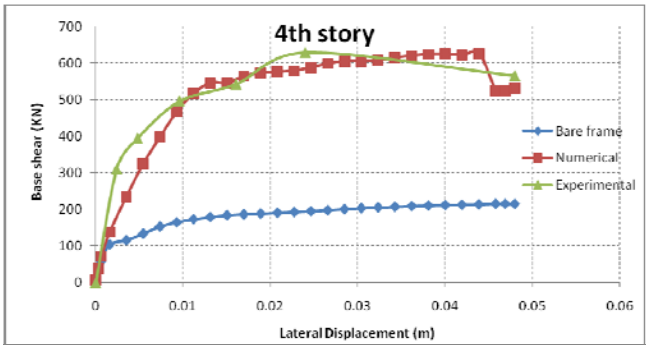

Figure 8 Push over results of 4th story

CRACK WIDTHS AND RESPONSE OF SPECIMENS

Cracks caused by earthquakes in various elements of a building are one of the most valuable factors for structural assessment. They are easily visible and are a good criterion of damage. In order to investigate the relationship between cracks and damage, cracks' width in RC columns and CB walls have to be measured quantitatively. In this analysis, flexural and shear cracks at the top and bottom of each column are schematically obtained at two stages shown in Figure 4. Also cracks in head joints as well as bed joints in the CB wall are obtained regarding their orientations at the aforesaid drift. The length of cracks is not important in the proposed model of assessment, but the largest width of cracks. This is done by measuring the difference of displacement in x and y directions of each pair of nodes. In this study, to quantitatively measure the width of cracks, 6 pairs of points in the infill wall are selected by dividing the diameter of infill into 4 sections and drawing perpendicular lines from them until they reach the edges of the infill wall. The differences between the displacements of the points in each pair are calculated. Figure 10 shows the mechanism of measuring cracks in the CB infill.

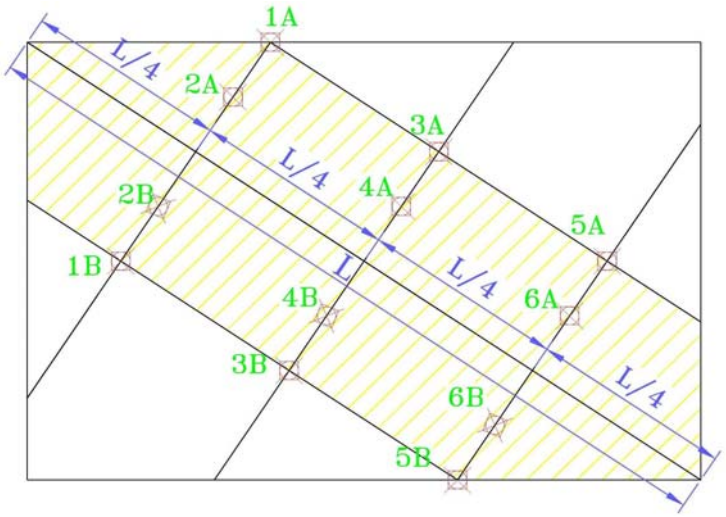

Figure 10 Crack width measurement concept

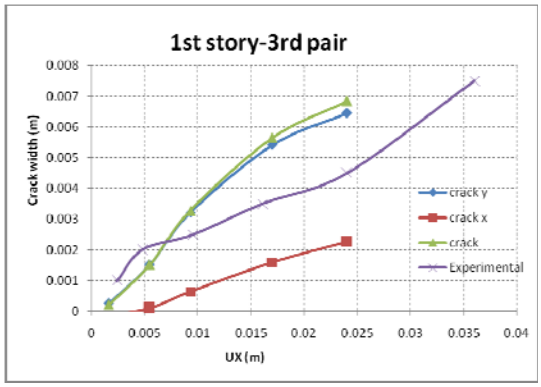

Figure 11 Crack width for model I1, node pair 3

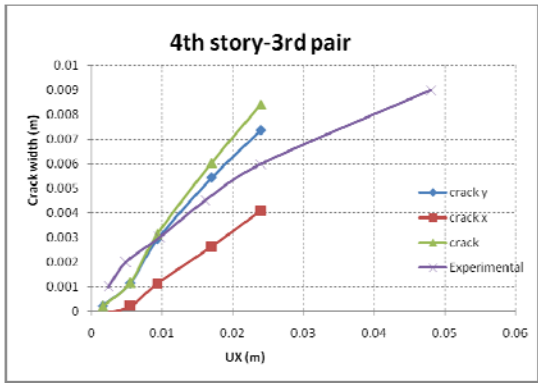

Figure 12 Crack width for model I4, node pair 3

CRACK WIDTH IN CB WALL AT PEAK LOAD

The relationship between lateral displacement and crack width in CB wall at the last peak of each step is plotted in Figures 11 and 12. As it is illustrated in these figures, the numerical simulation and the cracking measurement concept can acceptably measure cracks width in each stage, but slightly overestimate the crack widths in the final stages. Furthermore, sine the total crack width is almost equal to the vertical crack width, it can be concluded that many major cracks happen in vertical direction, hence horizontal movement. However, in the 4th story, the contribution of horizontal crack in the total crack width is more than in the 1st story based on its flexural behavior. Considering the inclinations of the cracks in Figure 4, it would be obvious that the main failure criterion of collapse is stair-stepped diagonal cracking which is in agreement with the experimental results. Figure 13 illustrates crack widths in the 1st and 4th stories in different node pairs. It is concluded that crack widths in the middle of the in infill wall (node pairs 3 and 4) is greater than other areas. Also, in node pairs 2,4 and 6, this difference is more obvious. So it can be inferred that major cracks have been concentrated in the middle of the infill close to diameter, while in the upper and lower parts of the infill, cracks are uniformly propagated around the diameter of the infill. In addition, crack width in the locations close to the diameter of the infill in the upper and lower parts are equal, but in the further regions from the diameter, (node pairs 1 and 5), the difference becomes apparent.

RELATION OF RESIDUAL DEFORMATION AND SEISMIC CAPACITY

The residual seismic capacity corresponding to each rotation angle can be numerically captured by the peak point of hysteresis figure for models I1 and I4. For this purpose, the ultimate drift angle should be defined. In this case R_u can be defined as drift angle corresponding to a percentage of the peak load in the hysteresis figure. In this way, the ductility factor for each model can be calculated.

In order to have a parameter which can represent the post-elastic behavior in terms of energy dissipation, the seismic capacity reduction factor η is defined as:

$$\eta = \frac{E_r}{E_T} = \frac{E_r}{(E_d + E_r)} \quad (3)$$

Where E_T is the initial or pre-earthquake seismic capacity, E_d is the dissipated energy or seismic capacity, and E_r is the residual energy capacity. For more information, readers are referred to [Choi et al., 2006]

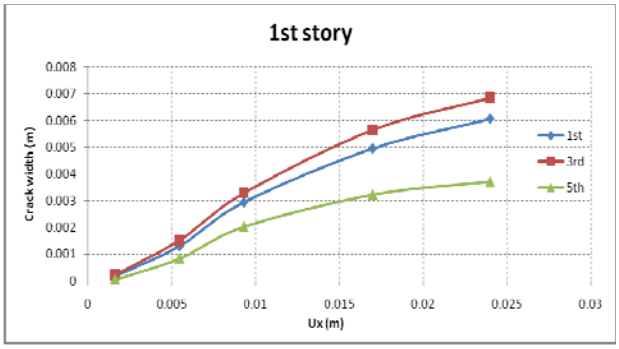

(a)

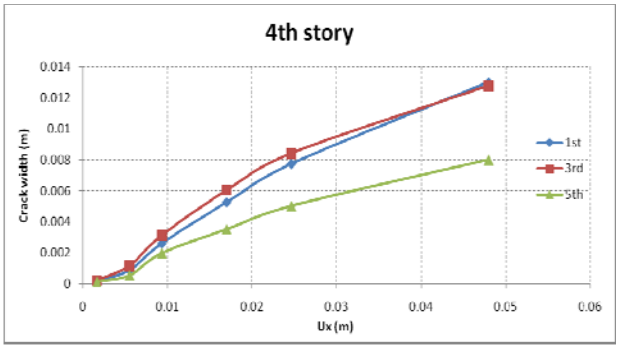

(c)

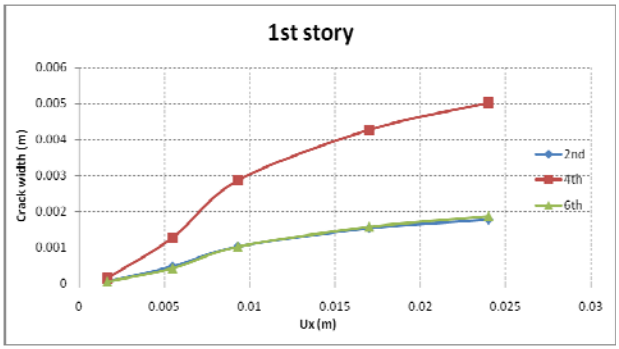

(b)

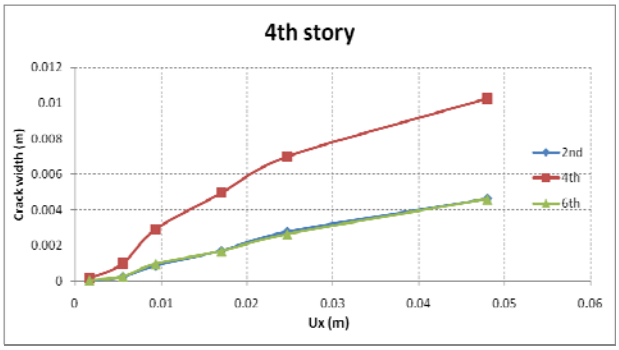

(d)

Figure 13 Crack widths (m) vs. lateral displacements (m) in different node pairs in the 1st and 4th stories

CONCLUSIONS

Masonry infills improve the strength of the combined systems as well as increase their stiffness. In this article, URM infill article inside RC frames were modeled numerically and the cracks widths in different stages were calculated. Without applying crushing capability, the models showed no softening behavior. Although the infill in the 4th story added less strength to the combined system when compared to the 1st story, it was more effective which increased the strength of the system up to 3 times. The remainder of the analyses was done according to push-over pattern for saving computational costs. It was concluded that crack widths are greater inside the infill walls near the diameter. Moreover, cracks, especially at the 1st story, are almost vertical and by considering crack patterns, the main failure mechanism is stair-stepped diagonal cracking. Although being a macro model and assuming the masonry to be a homogeneous material, the model is capable of determining the different modes of failure as well as the behavior of the combined system. The main advantage of this model is simplicity over the micro modeling and lesser cost of analyzing.

REFERENCES

1. Abu-Lebdeh, T.M., and Voyiadjis, G.Z., 1993, “Plasticity-damage model for concrete under cyclic multiaxial loading,” Journal of Engineering Mechanics, ASCE, 119(7), 1465-1484.
2. Chen, Yi-Hsin, 2003, “Seismic Evaluation of RC Buildings Infilled with Brick Walls”, PhD thesis, National Cheng- Kung Univ., Tainan, Taiwan,in Chinese.
3. Choi H., Nakano Y. and Sanada Y., Seismic Performance and Crack Pattern of Concrete Block Infilled RC Frames, Institute of Industrial Science, University of Tokyo, Bulletin of ERS No. 38, 2005
4. Choi H., Nakano Y. and Takahashi N., Residual Seismic Capacity of RC Frames with Unreinforced Block Wall Based on Their Crack Widths, Institute of Industrial Science, University of Tokyo, Bulletin of ERS No. 39, 2006
5. Del Piero, G., 1989, “Constitutive equation and compatibility of the external loads for linearly elastic masonry-like materials,” Meccanica 24, 150-162.
6. Dhanasekar, M., and Page, A.W., 1986, "The influence of brick masonry infill properties on the behavior of infilled frames." Proceedings of the Institute of Civil Engineers , Part 2, 81, Dec., 593-605.
7. Dhanasekar, M., Kleeman, P.W., and Page, A.W., 1985, "Biaxial Stress-Strain Relation for Brick Masonry." Journal of Structural Engineering , ASCE, 111(5), May.
8. Fanning, P., Nonlinear Models of Reinforced and Post-tensioned Concrete Beams, Electronic Journal of Structural Engineering, 2 (2001):111-119
9. Fuschi, P., Giambanco, G., and Rizzo, S., 1995, “Nonlinear finite element analysis of notension masonry structures,” Meccanica, 30(3), 233-249.
10. Gere, J. M. and Timoshenko, S. P., Mechanics of Materials, PWS Publishing Company, Boston, Massachusetts, 1997.
11. Hsieh, S.S., Ting, E.C., and Chen, W.F., 1988, “ Application of a plastic-fracture model to concrete structures,” Computers and Structures, 28(3), Pergamon, 373-393.
12. Kachlakev, D., Miller T., Finite Element Modeling of Reinforced Concrete Structures Strengthened with FRP Laminates, Final Report, SPR 316, for Oregon Department of Transportation Research Group and Federal Highway Administration, May 2001
13. Kent D.C., Park, R., Flexural members with confined concrete, Journal of the Structural Division, ASCE, Vol. 97, ST7, July 1971, pp. 1969-1990
14. Lee, J.S., Pande, G.N., Middleton, J., and Kralj, B., 1996, “Numerical modeling of brick masonry panels subject to lateral loadings,” Computers and Structures, Vol. 61, No. 4, Pergamon, 735-745.
15. Liauw, T.C., and Lo, C.Q., 1988, “Multibay infilled frames without shear connectors,” ACI Structural Journal, ACI, U.S.A. July-Aug 1988, 423-428.
16. Litton, R. W., 1974, “A Contribution to the analysis of concrete structures under cyclic loading,” PhD thesis, University of California, Berkeley.
17. Lopez J, Oller S, Onate E, Lubliner J. A homogeneous constitutive model for masonry. Int J Numer Methods Eng 1999;46: 1651–71.
18. Lotfi, H.R., and Shing, P.B. (1991). "An Appraisal of Smeared Crack Models for Masonry Shear Wall Analysis," Computers and Structures, 41(3), 413-425.
19. Lourenco, P. B. (1996). Computational strategies for masonry structures. PhD thesis, Delft University, Netherlands
20. Mehrabi AB, Shing PB, Shuller MP, Noland JL, +330, Experimental Evaluation of Masonry-Infilled RC Frames, Journal of Structural Engineering ASCE : 122(3) : 228-237
21. Mehrabi AB, Shing PB, 1997, Finite Element Modeling of Masonry-Infilled RC Frames, Journal of Structural Engineering ASCE : 123(5) : 604-613
22. Mostafaei H. and Kabeyasawa T., Effect of Infill Masonry Walls on the Seismic Response of Reinforced Concrete Buildings Subjected to the 2003 Bam Earthquake Strong Motion : A Case Study of Bam Telephone Center, Bulletin of Earthquake Research Institute, The University of Tokyo, Vol. 79 (2004), pp 133-156
23. Nakano Y., Choi H., Sanada Y. and Yamauchi N., Seismic Test of Concrete Block Infilled Reinforced Concrete Frames, Institute of Industrial Science, University of Tokyo, Bulletin of ERS No. 37, 2004
24. Ramalho M.A., Taliercio A., Anzani A., Binda L., Papa E., A Numerical Model for the Description of the Nonlinear Behaviour of Multi-leaf Masonry Walls, Advances in Engineering Software, 2007
25. Rots, J.G., and Borst, R, 1987, “Analysis of mixed-mode fracture in concrete,” Journal of Engineering Mechanics, ASCE, 113(11), 1739-1758.
26. Samarasinghe, W., Page, A. W. and Hendry, A. W. (1981). "Behaviour of masonry shear walls."The Structural Engineer Vol.59B(3): pp.42-48.
27. Schmidt, T., 1989, “An approach of modelling masonry infilled frames by the f.e. method and a modified equivalent strut method,” Darmstadt Concrete, Annual Journal on Concrete and Concrete Structures, Darmstadt University, Darmstadt, Germany.

28. Seim, W. (1994). Isotropic or anisotropic Simulation of inplane loaded masonry structures close to reality. 10th International Brick/Block Masonry Conference, Calgary, Canada, July 5-pp.77-86
29. Senthivel R., Lourenco P.B. and Vasconcelos G., Analytical Modeling of Dry Stone Masonry Wall Under Monotonic and Reversed Cyclic Loading, Structural Analysis of Historical Constructions, New Delhi 2006
30. Shing PB, Mehrabi AB, 2002, Behaviour and analysis of masonry-infilled frames, Prog. Struct. Engng Mater. 2002; 4:320–331
31. Stevens, D.J., and Liu, D., 1992, "Strain-based constitutive model with mixed evolution rules for concrete," Journal of Engineering Mechanics, ASCE, 118(6), 1184-1200.
32. Tavarez, F.A., (2001), "Simulation of Behavior of Composite Grid Reinforced Concrete Beams Using Explicit Finite Element Methods," Master's Thesis, University of Wisconsin-Madison, Madison,Wisconsin.
33. William, K.J. and Warnke, E.D. "Constitutive Model for the Triaxial Behaviour of Concrete", Proceedings of the International Association for Bridge and Structural Engineering, 1975, 19, p.174, ISMES, Bergamo, Italy
34. Willam, K., Pramono, E., and Sture, S., 1987, " Fundamental issues of smeared crack models,"SEM/RILEM International Conference on Fracture of Concrete and Rock, Houston, TX, June, Shah and Swartz, Editors.
35. Yazdani, S., and Schreyer, L., 1990, "Combined plasticity and damage mechanics model for plain concrete," Journal of Engineering Mechanics, ASCE, 116(7), 1435-1450.